ELSEVIER

Thermochimica Acta 291 (1997) 131–140

thermochimica acta

Reduction of tungsten oxides with carbon monoxide

Dean S. Venables, Michael E. Brown*

Department of Chemistry, Rhodes University, Grahamstown 6140, South Africa

Received 13 November 1995; received in revised form 29 January 1996; accepted 21 July 1996

Abstract

The reduction of WO_3 with CO was studied using thermogravimetry, evolved gas analysis, X-ray powder diffraction, and scanning electron microscopy. The intermediate phases $W_{20}O_{58}$, $W_{18}O_{49}$, and WO_2 were observed in the reduction. The final product of the reduction with CO was WC, compared with the tungsten formed when hydrogen and/or carbon was used. The reactant-to-product gas ratio has a considerable influence on the reactions taking place. The morphology of the sample was characterised at different stages of the reduction.

The kinetics and mechanism of the reduction of WO_3 with CO were studied in isothermal experiments, from 650 to 900°C. Reduction occurred at a phase boundary with an activation energy of 40 kJ mol^{-1}. The reduction of WO_2 was studied under similar conditions. The reaction also occurred at a phase boundary and had an activation energy of 62 kJ mol^{-1}. © 1997 Elsevier Science B.V.

Keywords: TG; EGA; Reduction of WO_3; Carbon monoxide

1. Introduction

The reduction of metal oxides with carbon usually occurs by way of CO formation as an intermediate. Thus, the reduction of tungsten oxides could be expected to proceed as follows:

$$WO_{x(s)} + CO_{(g)} \leftrightarrow WO_{y(s)} + CO_{2(g)} \quad (1)$$

(where $x > y$), and

$$C_{(s)} + CO_{2(g)} \leftrightarrow 2CO_{(g)} \quad (2)$$

The reduction of tungsten oxides with CO was thus studied so that the results could be compared with those for reduction with carbon [1,2].

*Corresponding author. Tel.: 0461 31 8254/5; fax: 0461 2 5109; e-mail: chmb@warthog.ru.ac.za.

PII S0040-6031(96)03068-7

2. Experimental

2.1. Materials

As in earlier experiments [1,2], namely: WO_3 (98% pure, Saarchem, 53–75 μm mesh); WO_2 was prepared by reducing WO_3 at 800°C under hydrogen which had been bubbled through water. $W_{18}O_{49}$ was prepared in a similar manner at 700°C. CO and CO_2 were supplied by Fedgas.

2.2. Equipment and techniques

The thermal analysis equipment, the tube furnace system and the experimental procedures were as described [1,2].

3. Results and discussion

Isothermal TG and DTG curves for the reduction of WO_3 with CO over the 650–900°C temperature range are shown in Figs. 1 and 2, respectively. The final product of the reaction was determined by XRD to be WC.

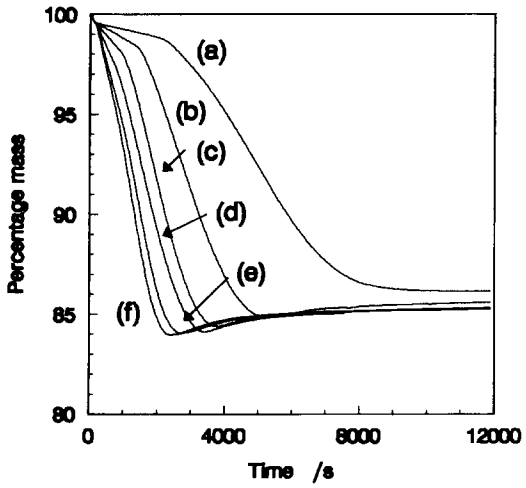

Fig. 1. Isothermal TG curves for the reduction of WO_3 with CO at a flow rate of 600 ml min^{-1}: (a) 650; (b) 700; (c) 750; (d) 800; (e) 850; and (f) 900°C.

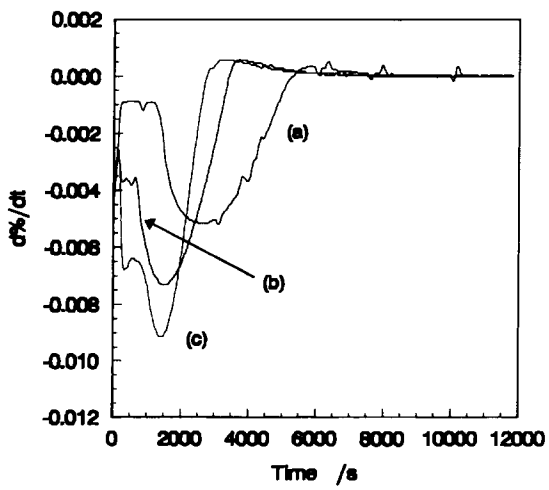

Fig. 2. Isothermal DTG curves for the reduction of WO_3 with CO at a flow rate of 600 ml min^{-1}: (a) 700; (b) 800; and (c) 900°C.

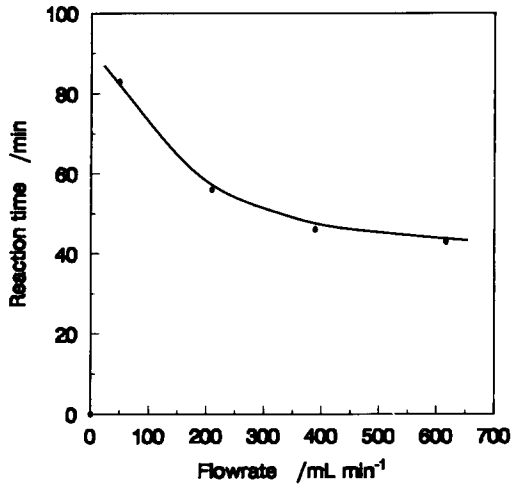

Fig. 3. The effect of flow rate on the time for complete reduction of WO_3 with CO.

The reaction was quite sensitive to the flow rate of CO, as is shown in Fig. 3. A temperature calibration of the TG performed at higher flow rates indicated a slight decrease (up to 10°C) in temperature registered by the furnace thermocouple. At flow rates above the critical value (i.e. the flow rate above which the transfer of gases to or from the solid is no longer rate-dependent), the reaction could be broadly divided into two steps: a small initial mass loss, and a second step with a much larger mass loss. (These mass losses occurred after an initial decrease of about 0.4% in mass while heating to the reaction temperature.) A small gain in mass after the second step was recorded at all temperatures above 650°C. This increase in mass took place at a moderate rate for a short while, but then decreased to a slow, constant rate. The constant mass gain almost certainly results from the deposition of carbon by the reverse of reaction (2). Similar observations were reported by Basu and Sale [3].

The first step appeared to be of zero order up to 750°C, and the products were $W_{20}O_{58}$ and $W_{18}O_{49}$. The mass loss for this step increased with temperature, and thus the composition of the sample at the end of this step probably varied from predominantly $W_{20}O_{58}$ at 650°C, to predominantly $W_{18}O_{49}$ at 750°C. From 800 to 900°C, the first stage of the process was still distinguishable by its lower rate of mass loss compared with the main reaction. An examination of the

rate of mass loss showed that this initial step actually consisted of two small maxima, suggesting that the reaction took place in discrete steps. The second step of the reaction corresponded to a large mass loss, and the curve of the rate of mass loss against time showed a single peak. Thus, this second step – the reduction from $W_{20}O_{58}$ and $W_{18}O_{49}$, to WC – appeared to take place in a single stage.

To determine the composition and morphology of the sample during the course of the reaction, a number of experiments were carried out at 900°C in which the reaction was interrupted at different times. The extent of reaction during cooling was probably small because the sample cooled rapidly. The samples were examined at room temperature and were assumed to be reasonably representative of the composition and morphology of the samples at the time the reaction was interrupted.

Table 1 lists the colour of the samples and the phases identified by XRD in each sample. No more than two phases were observed in any sample. The quantity of each phase present could thus be estimated from the mass loss at the end of the experiment (excluding the initial mass loss on heating). A further experiment, interrupted after about 27 min at 800°C, indicated that only α-W and $W_{18}O_{49}$ were present in significant quantities in the sample ($\sim$ 30% α-W and 70% $W_{18}O_{49}$).

From the phases observed up to 8 min, and their relative quantities, it seems reasonable to predict the following initial steps in the reduction:

$$WO_3 \xrightarrow{(1)} W_{20}O_{58} \xrightarrow{(2)} W_{18}O_{49}$$

The product of the steps (1) and (2) in the reduction therefore appears to be $W_{18}O_{49}$, and perhaps includes some $W_{20}O_{58}$ at temperatures below 800°C. Thereafter, $W_{18}O_{49}$ is directly reduced to α-W, as observed after 16 min (Step (3)):

$$W_{18}O_{49} \xrightarrow{(3)} \alpha - W$$

After about 29 min, the sample contained no $W_{18}O_{49}$ but consisted predominantly of WO_2 and lesser amounts of α-W. This means that either $W_{18}O_{49}$ was also reduced to WO_2 by the reaction step (4):

$$W_{18}O_{49} \xrightarrow{(4)} WO_2$$

which became the dominant reaction, or that step (3) occurred together with the reaction of α-W and $W_{18}O_{49}$ to give WO_2:

$$11W + 2W_{18}O_{49} \leftrightarrow 49WO_2$$

The second possibility is unlikely to be significant because the reaction of tungsten with tungsten oxides to form oxides of intermediate stoichiometry is extremely slow compared with the relatively short reduction time with CO. (For example, the reaction of tungsten with WO_3 to form WO_2 takes 40 h at 950°C [4].)

What then determines the relative importance of steps (3) and (4)? At 800°C, WO_2 was not observed after $\sim$27 min, which suggests that Step (4) is not significant at this temperature. Step (4) was observed only at a relatively high reaction rate, and consequently at relatively high partial pressures of CO_2. A graph of the CO/CO_2 equilibrium ratios for some of the reactions in the system (Fig. 6 in [1]) shows that the reduction of $W_{18}O_{49}$ to α-W (step (3)) requires a higher CO/CO_2 ratio than the reduction of $W_{t8}O_{49}$ to WO_2 (step (4)). Thus, at the start of the reduction (when the CO/CO_2 ratio in the system is high), step (3) dominates the reduction sequence, but is suppressed as the amount of CO_2 increases in the atmosphere around the sample. Thereafter, the reaction proceeds mainly by step (4).

Table 1
Intermediate phases in the isothermal reduction of WO_3 in CO at 900°C

Time (min)	Mass loss (%)	Colour	Phases present	Estimated amount	
3	0.4	Blue-green	WO_3	100%	
6	1.5	Deep blue	$W_{20}O_{58}$	70%	
			$W_{18}O_{49}$	30%	
8	2.4	Dark purple	$W_{20}O_{58}$	Traces	
			$W_{18}O_{49}$	100%	
16	5.0	Deep purple	$W_{18}O_{49}$	90%	
			α-W	10%	
29	10.9	Not recorded	WO_2	70%	
			α-W	30%	
47	16.2	Grey	WC	100%	
>120	15.4	Grey	WC		100%

The transformation of WO_2 to WC may be either indirect, namely

$$WO_2 \xrightarrow{(5)} \alpha - W$$

followed by:

$$\alpha - W \xrightarrow{(6)} WC$$

or direct, according to

$$WO_2 \xrightarrow{(7)} WC$$

Higher CO/CO_2 ratios are required for step (6) to occur below 850°C. Consequently, the tungsten formed during the reduction will probably form WC only when the reaction is almost complete. There was a mass gain towards the end of the reaction which was more rapid than the subsequent deposition of carbon. This mass gain can be attributed to step (6), which is the only reaction resulting in an increase in mass. An experiment to investigate the carburisation of tungsten (step (6)) at 900°C (not illustrated) showed that the reaction was initially rapid, but slowed down markedly after a mass gain of about 1.2%.

The reaction scheme inferred from the above observations is shown in Fig. 4.

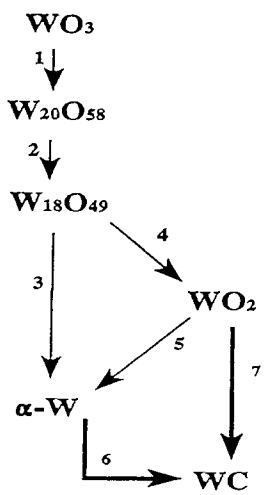

Fig. 4. The reaction scheme for the reduction of WO_3 with CO at 900°C and a high flow rate.

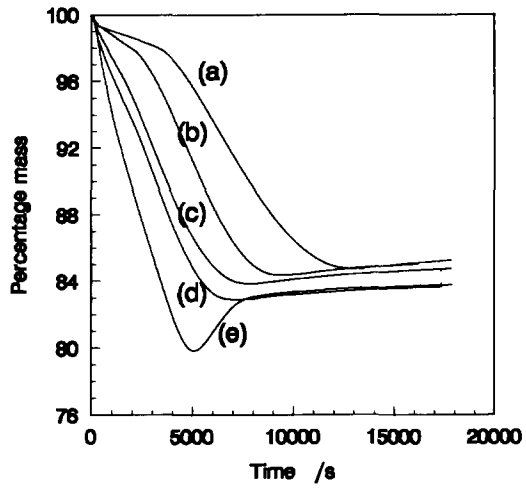

Fig. 5. The isothermal reduction of WO_3 with CO at a flow rate of 50 ml min^{-1}: (a) 700; (b) 750; (c) 800; (d) 850; and (e) 900°C.

At a flow rate of 50 ml min^{-1} the reduction was appreciably slower than at 500 min^{-1} (Fig. 5), indicating that mass transport controlled the rate of reaction at low flow rates (Fig. 3). Because the sample was small, reacted slowly, and the gas was pure CO, the reaction rate could not be limited by a lack of CO at the sample. Instead, the reaction rate was probably limited by the reducing potential of the gas which decreased as CO_2 formed in the reduction.

Since the calculated CO/CO_2 equilibrium ratio for the reduction of WO_3 to WO_2 is small, the first stage of reaction might be limited by some other factor associated with the reduction. Nonetheless, the first stage of the reaction was also much longer at low flow rates than at high flow rates, which suggested that the reverse reaction was significant at low flow rates. The temperature dependence of the first stage of the reaction was greater than that of the main stage. Thus, at high temperatures and low flow rates, the rate of the first stage of the reaction surpassed that of the second stage (Fig. 5), possibly because the rate of the second stage was more affected by the higher CO/CO_2 equilibrium ratio.

At 900°C, the maximum mass loss corresponded to that expected for the formation of metallic tungsten, and was followed by a considerable gain in mass as carburisation took place. (This mass gain was larger than that observed in a separate experiment to study

the carburisation of a sample of tungsten powder.) The maximum mass loss was much smaller at high flow rates, thereby indicating the important influence of the CO/CO_2 ratio on the reaction.

During the reductions of WO_3 and WO_2 with CO, the reactions appeared to proceed from the bottom of the sample upwards, and from the sides inwards. Often the top centre of the surface retained the original colour of the sample for a considerable length of time, whereas the sides and bottom of the powder layer were the colour of the product. This is contrary to the expectations, because the atmosphere at the bottom of the powder layer tends to be more oxidising than that at the surface, where the CO_2 produced is removed and replaced by CO. When iron powder was heated under similar conditions it increased in mass, indicating that traces of oxygen were in the system. Small amounts of oxygen would explain the observed tendency for the reaction to start from the bottom of the sample.

3.1. Isothermal reduction of WO_2 with CO

The isothermal reduction of WO_2 with CO was also studied at a high flow rate, and the results are shown in Figs. 6 and 7. An induction period was observed over the entire temperature range studied. No mass loss

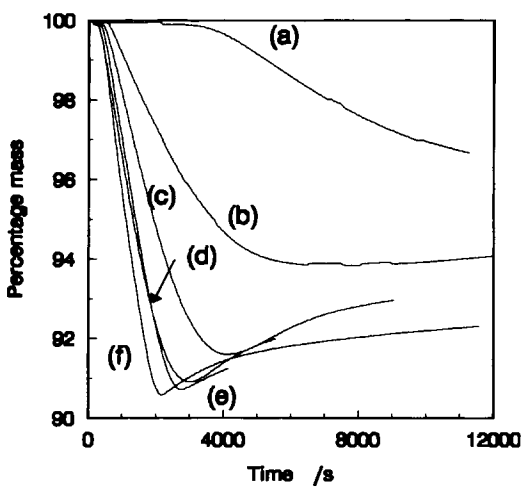

Fig. 6. Isothermal TG curves for the reduction of WO_2 with CO at a flow rate of 600 ml min^{-1}: (a) 650; (b) 700; (c) 750; (d) 800; (e) 850; and (f) 900°C.

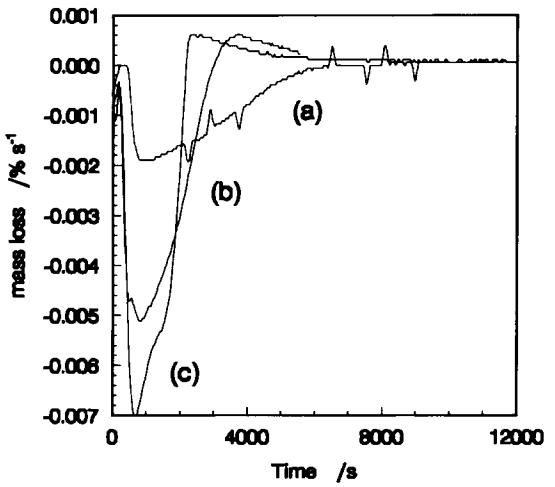

Fig. 7. Isothermal DTG curves for the reduction of WO_2 with CO at a flow rate of 600 ml min^{-1}: (a) 700; (b) 800; and (c) 900°C.

accompanied this period, which suggested that nucleation took place before the reaction proceeded. The rate of mass loss showed that the main reaction takes place in a single stage at and below 750°C. At 850 and 900°C, however, there were indications of overlapping peaks in the rate of mass loss curve. These could indicate that there are two reaction paths in the system, possibly the two alternative paths whereby WO_2 can be reduced to WC, that is, either step (7), or steps (5) and (6).

In an attempt to establish the reaction paths more precisely, the reduction of WO_2 with CO was interrupted after 12 min at 900°C and after 25 min at 850°C. These times correspond approximately to the first and second peaks in the rate of mass loss curve. At 900°C, the sample consisted primarily of WO_2, with small amounts of both α-W and WC also present, thus suggesting occurrence of both pathways. At 850°C, the sample was predominantly WC, with smaller quantities of WO_2, implying that either step (6) is rapid compared to step (5), or that step (7) dominates the reduction sequence.

3.2. Morphological changes

The morphologies of the samples interrupted during reduction were examined using SEM. After 3 min, the sample was very similar to the starting WO_3, but

reduction for a slightly longer time resulted in marked changes. The smooth surface of the WO_3 particles was converted to a surface covering of small needles after about 6 min. These needles are typical of the formation of $W_{18}O_{49}$, and were quite flat and randomly oriented on the face of the pseudomorph. Extensive cracking was apparent. The morphology of the particles observed after 6 min was retained during the course of the reduction, indicating that the strong tendency of $W_{18}O_{19}$ to form needles dictates the morphology of the subsequent phases and also that of the final product. The pseudomorphs appear to increase in porosity as the reaction progresses, as is expected from the decrease in the molar volume of the more reduced phases. The well-defined shape of the needles was lost somewhat towards the end of the reaction and the needles appeared to be shorter and more rounded.

A similar morphology was observed for the final reduction product at 800°C. However, at 650°C the development of the needles appeared to be retarded and the surface of the particles was only slightly textured. The product of the reduction of WO_2 at 650°C was unchanged from the WO_2 starting material. Particles from the carburisation of tungsten were very similar to the starting material.

3.3. Kinetic analysis

As the reaction scheme in Fig. 4 shows, there are a number of possible reaction steps in the process. This complicates the kinetic analysis, because different reactions generally occur at different rates, simultaneously or consecutively, with different temperature dependencies. The kinetics of the reduction of WO_2 (which has fewer reaction steps) is considered before examining the kinetics of the reduction of WO_3.

3.4. Reduction of WO_2 with CO

WO_2 may be reduced (a) directly to WC, or (b) via α-W. The expected mass loss for formation of W is 14.83% of the original mass of WO_2. In none of the experiments illustrated in Fig. 6 is this value even remotely approached. The maximum recorded mass losses and the estimated final mass losses after carburisation, for these experiments, are given in Table 2.

Table 2
Maximum mass losses in the reduction of WO_2 by CO

Temperature (°C)	Maximum mass loss (%)	Final mass loss (%)
650	—	—
700	6.2	6.2
750	8.4	7.1
800	9.1	7.9
850	9.3	(Incomplete)
900	9.5	8.4

Complete conversion of WO_2 to WC would correspond to a mass loss of 9.3%. The final mass losses after carburisation fall well short of the above value, although the maximum mass losses approach this value at and above 800°C. Incomplete reduction of WO_2 is probably the main reason for the smaller than expected mass losses, although carbon deposition in a separate process may also decrease the observed mass losses slightly. Basu and Sale [3] have reported similar results for the reduction of WO_2.

There are three main possibilities in considering the kinetics of the reaction:

1. Path (a) is very slow compared to the alternative path (b).
2. Path (a) is the more rapid path.
3. Both pathways contribute significantly to the formation of WC as the final product.

No evidence from the WO_2–CO experiments indicates that path (b) is dominantly rapid under the conditions investigated.

The process may be considered as being composed of a mass loss and a mass gain component, which when combined result in the experimental mass loss curve. The limits of the mass loss component fall between 9.3% (for conversion to WC with no intermediate tungsten formed) and 14.8% (for complete conversion to tungsten with no WC being formed). Depending on the extent to which tungsten is formed, the carburisation of tungsten results in an increase in mass of up to 5.6% of the original mass of WO_2. If the experimental mass loss curve could be deconvoluted to give the separate mass loss and mass gain curves, then in principle the kinetics of these components could be analysed separately. However, such a procedure requires detailed knowledge of the course of

reaction. Therefore, a kinetic analysis can only proceed on the basis of several assumptions.

There are essentially three ways to define α:

1. $\alpha = 1$ at the final mass loss after carburisation.
2. $\alpha = 1$ at the theoretical mass loss for the conversion of WO_2 to WC.
3. $\alpha = 1$ at the maximum mass loss.

Of these options, (1) is the least satisfactory, since α will reach unity well before the final mass loss is attained, when the reaction is obviously incomplete. Option (2) is a better estimate of α from a theoretical point of view, although the same problem arises as in the first option when the maximum mass loss exceeds 9.3% (as happens at 850 and 900°C). Furthermore, it is perhaps better to measure the extent of reaction in terms of when the reaction ends, rather than at the complete conversion of reactants into products. This is especially true if the equilibrium amount of the reactants is significant, or if other stable phases are formed during the reaction.

The third option seems to give the most useful definition of α. As has been discussed, the carburisation of tungsten is more likely to occur towards the end of reaction, so that at the maximum mass loss all the reactions in which mass is lost will probably be virtually complete. According to this definition, α is essentially a measure of the extent to which the reactions involving mass losses are complete, and excludes the contribution of carburisation to the overall process. The effect of carbon deposition on the process is ignored in the kinetic analysis, since the mass gains are quite small. Furthermore, the higher CO_2 partial pressure in the system during the main stages of reaction will suppress the deposition of carbon to some extent.

The induction period and short acceleratory part of the reaction are usually indicative of the formation and growth of nuclei, and suggest that the process is not exclusively controlled by diffusion or by reaction at a boundary between two phases. Another possible explanation for the acceleratory period is that the reaction did not occur uniformly over the sample, but started at the bottom of the sample and progressed upwards, as was observed. If this is the case, the acceleratory period is caused by the temporal increase in the amounts of powder layer contributing to the reaction.

Table 3
The correlation coefficients for the kinetic models which gave the best fit to the experimental data for the reaction of WO_2 with CO over the $0.05 < \alpha < 0.99$ range

Temperature (°C)	R2	R3	A2	A3	Prout–Tompkins
700	0.9977	0.9972	0.9979	0.9930	0.9898
750	0.9979	0.9854	0.9924	0.9920	0.9779
800	0.9968	0.9821	0.9904	0.9929	0.9785
850	0.9880	0.9648	0.9811	0.9914	0.9733
900	0.9859	0.9607	0.9792	0.9891	0.9698

The reaction kinetics were analysed by comparing the linearity of the kinetic models [5], using the experimental α, t data. Since the α, t curves have a brief acceleratory period, the sigmoid group of models (i.e. Avrami–Erofe'ev equation and the Prout–Tompkins model) were tested and fitted the data reasonably well. The deceleratory models were also examined since the major portions of the α, t curves were deceleratory. Table 3 lists the correlation coefficients, r^2, determined for the models which gave the best fit to the data at the temperatures studied.

The experimental curve is compared with the curves predicted by the R2 and A2 models at 750°C in Fig. 8. As might be expected, the R2 model fits the experi-

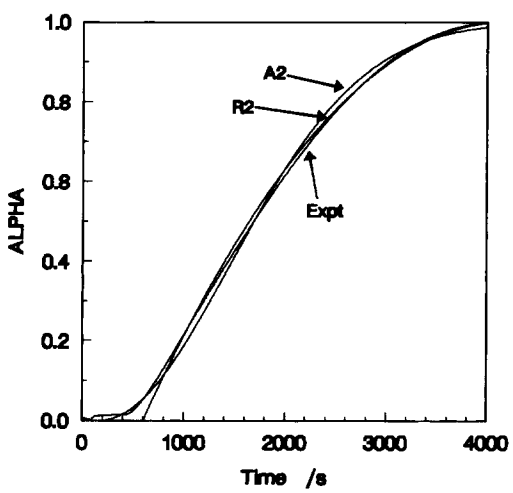

Fig. 8. Comparison of the experimental α values, for the reduction of WO_2 with CO at 750°C, with those calculated using the R2 and A2 models.

mental data over the main deceleratory region better than the A2 and A3 models. An Arrhenius plot using the values of the rate coefficients determined by the R2 model, gave an activation energy of 62 ± 5 kJ mol^{-1} and a frequency factor of 3.9 ± 0.3 s^{-1}.

3.5. Reduction of WO_3 with CO

Unlike the case of WO_2, the reduction of WO_3 with CO took place in two main reaction stages. These stages were analysed separately for reactions below 800°C because: (1) the transition from the first to the second stage is readily identified; (2) the reaction products of the second stage are known ($W_{20}O_{58}$ and $W_{18}O_{49}$); and (3) the first stage of the reaction appears to take place in a single stage (up to 750°C).

From 800 to 900°C, only the kinetics of the second stage of the reaction were analysed. As with the reduction of WO_2, the reaction was assumed complete at the maximum mass loss. The α, t curve included both stages of the process because the first and second stages of the reduction could not be separated accurately. The error introduced by using a different starting point for the reaction is probably small since the mass loss of the first stage was only about 10% of the total mass loss. Table 4 lists the mass losses at the end of the first and second stages.

The first stage of the reaction took place at an approximately constant rate, which indicates a zero-order reaction. The correlation coefficients and the rate constants calculated for a zero-order reaction are listed in Table 5. An activation energy and frequency factor of 66 ± 2 kJ mol^{-1} and 2.41 ± 0.04 s^{-1}, respectively, were calculated for the first stage of reaction.

Table 4
The mass losses taken to be the end of the first and second stages of the reaction for the reduction of WO_3 with CO

Temperature (°C)	Mass lost from the starting mass (%)	
	First stage	Second stage
650	1.3	13.9
700	1.8	15.1
750	2.3	15.6
800	—	15.9
850	—	16.0
900	—	16.0

Table 5
The correlation coefficients and rate constants calculated for the first stage of the reduction of WO_3 by CO, for a zero-order reaction rate

Temperature (°C)	r^2	k (10^{-4} s^{-1})
650	0.9996	4.69
700	0.9985	7.42
750	0.9989	10.8

The reliability and meaning of the kinetic parameters are questionable when applied to a process involving a number of steps. In the reaction being studied, the process is probably:

$$WO_3 \xrightarrow{(1)} W_{20}O_{58} \xrightarrow{(2)} W_{18}O_{49}$$

as has been discussed. However, the extent to which this process is complete directly depends on temperature, and the extent to which steps (1) and (2) are complete is not known. If the product of first stage is $W_{18}O_{49}$, then it would be more accurate to calculate α assuming that $\alpha = 1.00$ at the mass loss expected for the formation of $W_{18}O_{49}$. Calculations using this definition of α gave an activation energy of 128 ± 6 kJ mol^{-1}, which differs considerably from the activation energy calculated previously.

Another method of calculating the rate constant for the process is from the reciprocal time of the induction period, which is independent of the mass loss. The results obtained using this method were very similar to those determined using the first estimate of α: the activation energy was 65.7 ± 0.2 kJ mol^{-1}, and the frequency factor was 2.67 ± 0.05 s^{-1}. These values support the assumption that the process was complete at the end of step (1).

From the above conclusions regarding the definition of α, and the observed variation in the mass loss at the end of the first stage, the zero-order behaviour of the process is probably attributable to the formation of $W_{20}O_{58}$ because step (1) could occur completely at the observed mass losses during the first stage. Furthermore, the reduction of WO_3 to $W_{20}O_{58}$ by hydrogen has also been reported to take place at a constant rate [6], which suggests that the nature of the process is

Table 6
The correlation coefficients of the R2 model and the zero-order rate equation. The R2 model was applied over most of the α, t curve; the zero-order rate equation was only applied over the middle of the curve

Temperature (°C)	Correlation coefficients	
	zero-order rate equation	R2 model
650	0.9998	0.9711
700	1.0000	0.9863
750	0.9996	0.9847
800	0.9998	0.9823
850	0.9998	0.9827
900	1.0000	0.9814

influenced more by the structure of the solids (especially that of $W_{20}O_{58}$) than by the particular reducing agent. Since the extent of reaction of the first stage represents the extent of formation of $W_{20}O_{58}$, the calculated activation energy of 65 kJ mol^{-1} is proposed to be that of the reduction of WO_3 to $W_{20}O_{58}$.

The greater mass loss at higher temperatures indicates the extent to which $W_{18}O_{49}$ is formed. The zero-order nature of the process appears to apply to the formation of $W_{18}O_{49}$ too, possibly because the formation of $W_{20}O_{58}$ and $W_{18}O_{49}$ occur in tandem.

For the second stage of reaction, the geometric models (especially R2) gave the best fit to the experimental data, although it was apparent that the middle of the α, t curve was approximately linear, i.e. a zero-order process. Table 6 lists the correlation coefficients for the R2 model and the zero-order rate equation at the temperatures studied.

Arrhenius plots using the rate constants calculated from the R2 model and the zero-order rate equation, gave an activation energy of 40 ± 7 kJ mol^{-1} and a frequency factor of $(3.7 \pm 0.6) \times 10^{-2}$ s^{-1} using the R2 model; and 33 ± 8 kJ mol^{-1} and $(2.0 \pm 0.4) \times 10^{-2}$ s^{-1} using the zero-order rate equation.

The good fit of the R2 model to the later stages of reduction suggests that the reaction occurred at a phase boundary which advanced inwards at a constant rate towards the end of the reduction. The beginning and middle of the reduction are less certain, and seem to involve some acceleratory process, perhaps nucleation and growth, or reaction starting from the bottom of the sample pan.

4. Discussion

Despite the difficulty in choosing a suitable definition of α, the kinetics were quite consistent for the reductions of WO_3 and WO_2. The good agreement of the geometric models suggests that the reaction occurs at an interface which advances into the particle. The induction period suggested that nucleation of the phase being formed may occur. The reduction was controlled by mass-transfer at low flow rates, as Basu and Sale [3] also found.

The kinetics of the reduction with CO are similar to those reported for the reduction with hydrogen [7]. In particular, Taskinen et al. [8] reported that the reduction of WO_2 with hydrogen fitted the R2 model, and an induction period during reduction with hydrogen has been observed by Charlton [9,10].

The initial zero-order reaction in the reduction of WO_3 is probably associated with the reduction of $W_{20}O_{58}$. If this is the case, then the constant rate at which $W_{20}O_{58}$ is formed may be related to the formation or migration of crystallographic shear planes in the WO_3 lattice.

The formation of α-W during the reduction may result either from reduction of $W_{18}O_{49}$ or of WO_2. Most carburisation takes place towards the end of the reaction, when the CO/CO_2 ratio is relatively high. Although the investigation into the carburisation of tungsten powder indicated that the reaction was very slow after about $\alpha = 0.20$, the tungsten produced during the reduction of tungsten oxides will probably be much more reactive and would be more likely to react to completion. The mass loss curves in the reductions of WO_3 and WO_2 and the results of Basu and Sale [3] suggest that this is the case.

The Arrhenius plots of the reductions of WO_3 and WO_2 are quite curved, possibly indicating that the reaction mechanism changes with temperature. This change may result from the variations in the structure of the particles at different temperatures. Alternatively, differences in the CO/CO_2 ratios at different temperatures may alter the reactions which take place during the overall process. If the reaction mechanism changes, then the activation energy will be higher at low temperatures than the calculated activation energy, and at high temperatures the activation energy will be lower than the calculated activation energy.

Acknowledgements

The authors acknowledge with gratitude the advice and assistance given by Karol Cameron, Ian Sutherland and Ian Porée of the Solid State Chemistry Group, AECI Chemicals Ltd., and financial support from AECI Chemicals Ltd. and the Foundation for Research Development.

References

[1] D.S. Venables and M.E. Brown, Thermochim. Acta, 282/283 (1996) 251..
[2] D.S. Venables and M.E. Brown, Thermochim. Acta, 282/283 (1996) 265..
[3] A.K. Basu and F.R. Sale, Metall. Trans. 9B (1978) 603.
[4] C.L. Rollinson, in J.C. Bailar, H.J. Emeléus, R. Nyholm and A.F. Trotman-Dickenson (Eds.), Comprehensive Inorganic Chemistry, Vol. 3, Pergamon, Oxford (1973) Chap. 4.
[5] M.E. Brown, D. Dollimore, and A.K. Galwey, in C.H. Bamford and C.F.H. Tipper (Eds.), Comprehensive Chemical Kinetics: Reactions in the Solid State, Vol. 22, Elsevier, Amsterdam (1980).
[6] P. Barret and L.C. Dufour, C. R. Acad. Sci. Paris 258 (1964) 2337.
[7] D.S. Venables and M.E. Brown, Thermochim. Acta 285 (1996) 361.
[8] P. Taskinen, P. Hytönen and M.H. Tikkanen, Scand. J. Metallurgy 6 (1977) 228.
[9] M.G. Charlton, Nature 152 (1952) 109.
[10] M.G. Charlton, Nature 174 (1954) 703.